nature COMMUNICATIONS

ARTICLE

https://doi.org/10.1038/s41467-019-11519-9 OPEN

Using B isotopes and B/Ca in corals from low saturation springs to constrain calcification mechanisms

M. Wall[1,2], J. Fietzke[1], E.D. Crook[3,4] & A. Paytan[4]

Ocean acidification is expected to negatively impact calcifying organisms, yet we lack understanding of their acclimation potential in the natural environment. Here we measured geochemical proxies ($\delta^{11}B$ and B/Ca) in *Porites astreoides* corals that have been growing for their entire life under low aragonite saturation (Ω_{sw}: 0.77–1.85). This allowed us to assess the ability of these corals to manipulate the chemical conditions at the site of calcification (Ω_{cf}), and hence their potential to acclimate to changing Ω_{sw}. We show that lifelong exposure to low Ω_{sw} did not enable the corals to acclimate and reach similar Ω_{cf} as corals grown under ambient conditions. The lower Ω_{cf} at the site of calcification can explain a large proportion of the decreasing *P. astreoides* calcification rates at low Ω_{sw}. The naturally elevated seawater dissolved inorganic carbon concentration at this study site shed light on how different carbonate chemistry parameters affect calcification conditions in corals.

[1] GEOMAR Helmholtz-Centre for Ocean Research Kiel, Marine Geosystems & Marine Ecology, Wischhofstr 1-3, 24148 Kiel, Germany. [2] Department of Palaeontology, University of Vienna, Althanstraße, 1090 Vienna, Austria. [3] Department of Earth System Science, University of California, Irvine, Croul Hall, Irvine, CA 92697-3100, USA. [4] University of California, Earth and Marine Science Building, 1156 High Street, Santa Cruz, CA 95064, USA. Correspondence and requests for materials should be addressed to M.W. (email: mwall@geomar.de)

Ocean acidification is projected to lead to negative effects on calcifying organisms, particularly tropical corals[1–3]. Our understanding of the potential fate of corals in the face of changing pCO_2 in the ocean is based primarily on controlled laboratory studies (e.g. refs. [4,5]), mesocosm studies mimicking coral community composition[6–8], alkalinisation versus carbon dioxide-enrichment studies in natural coral reef sites[9,10], and a number of field studies with naturally reduced calcium carbonate saturation state (Ω_{arag})[1,11–14]. These efforts have provided strong evidence that the calcification rates of a large number of coral species investigated to date will decline in response to projected pCO_2[15]. However, some studies also report that certain coral species were able to maintain high calcification rates or even benefit from elevated pCO_2[1,16–18], suggesting a high resilience potential of some coral species to changing carbonate chemistry[19]. Specifically, the ability of an organism to control the biomineralization process clearly determines its ecological and physiological success under reduced pH conditions[14]. The process of calcification in corals is linked to their ability to control the pH at the site of calcification (pH_{cf}) by removing protons out of the calicoblastic space between the tissue and skeleton, where calcification takes place[5]. This enables corals to sustain pH_{cf} well above seawater pH (pH_{SW})[5,19,20]. The physiological capacity of corals to control pH_{cf} may alleviate the decline in coral growth and increase coral resilience to future climate change[19]. Knowledge about internal calcifying fluid pH_{cf} in corals has been derived from a few direct measurements under the calcifying cell layer either using microsensors[21,22] or pH-sensitive dyes[5,23]. These studies confirmed an elevated pH_{cf} of between 0.4 and 2 pH units above ambient seawater in the calicoblastic space. Indirectly, boron isotopes ($\delta^{11}B$) of coral skeletons, which represent the pH_{cf} of the calcifying solution, also suggest an elevated pH_{cf} (e.g. refs. [19,24–26]). Boron isotopes are more readily accessible compared to direct measurements and have the additional benefit that they integrate pH_{cf} history over longer time periods[19,20,24,27]. Studies suggest that pH_{sw} is an important driver affecting pH_{cf} [25,28]. However, it was recently demonstrated that changes in seawater dissolved inorganic carbon (DIC) or total alkalinity (TA) can also affect pH_{cf} regulation[23]. Using B/Ca as a proxy for internal carbonate ion concentration ($CO_3^{2-}{}_{cf}$), provided geochemical evidence that corals can also modulate and adjust the internal DIC (DIC_{cf}) concentration. Together—the potential to upregulate DIC_{cf} and pH_{cf}—allows for higher carbonate ion concentrations at the site of calcification and hence a higher Ω_{cf} that facilitates calcification[29,30].

Over the last decade, a growing body of literature has provided evidence that corals subjected to daily and seasonally fluctuating environmental conditions are able to exert a stronger control over their internal physiological attributes, potentially allowing them to better cope with future changes (reviewed in ref. [31]). For instance, in situ flume experiments mimicking natural (daily, seasonal) fluctuating conditions coupled with future pCO_2 conditions showed that corals from acidified treatments could maintain a constant calcification pH_{cf} irrespective of changes in seawater pH_{sw}[27]. The authors argued that the fluctuating conditions the corals were exposed to likely favour this strong control on internal conditions. That year long experiment, however, cannot tell whether corals can maintain such strong control when exposed to reduced mean seawater aragonite saturation state (Ω_{sw}) for their entire life span. Corals living for their entire life under continuously low Ω_{sw} and variable environmental conditions can be used to test whether corals can maintain pH_{cf} homoeostasis over long time spans in their natural ecosystem with its complex biological interactions. Because many natural ocean acidification sites also show strongly fluctuating conditions[11,32,33] these settings may be ideal for testing the relationship between environmental variability and acclimation potential of corals to low Ω_{sw}[34].

Here we measured geochemical proxies in the upper most recently formed skeletal parts of *Porites astreoides* corals that were collected along a natural aragonite saturation gradient at submarine springs (locally known as ojos) in Puerto Morelos, Mexico[11]. These geochemical proxies ($\delta^{11}B$-derived estimates of pH_{cf} and B/Ca derived estimates of $CO_3^{2-}{}_{cf}$) allowed us to infer carbonate chemistry conditions at the site of calcification, which provide valuable new insights into the internal calcification regulation mechanisms in corals exposed to persistent low Ω_{sw}, as well as fluctuating carbonate chemistry conditions[33]. Our results, combined with bio-inorganic calcification models[19,30], identified critical regulation mechanisms and the inability of corals to fully acclimate to these conditions and sufficiently elevate their Ω_{cf} to sustain growth rates similar to the same species of corals growing at ambient Ω_{sw}.

Results

Natural conditions at the ojos. We used 12 cores from the coral *P. astreoides*: 5 cores collected from the centre of the low Ω_{sw} ojos and 7 from control present-day Ω_{sw} sites adjacent (within a few meters) to the ojos[11]. *Porites astreoides*, the species used in this study, represents one of only three calcifying coral species found growing within the discharge impacted area, while nine coral species are found nearby under ambient present-day Ω_{sw}. Previous studies indicate that although the abundance of *P. astreoides* was not significantly reduced at the low Ω_{sw} ojos, its growth rate (measured as net calcification) decreased significantly by 37% compared to the same species collected at control sites[11]. The control sites have a relatively consistent Ω_{sw} (on average: 3.92 ± 0.03 sd) year round compared to the ojos where Ω_{sw} is always <2 and ranges from 0.77 to 1.85 (on average: 1.49 ± 0.14 sd, Supplementary Table 1 [11]).

Skeletal $\delta^{11}B$ and thus pH_{cf} as a function of Ω_{sw}. The $\delta^{11}B$ in the 12 corals analysed ranged from 23.1‰ to 27.6‰, with slight but significantly lower values for corals affected by the ojo discharge where Ω_{sw} was low (Fig. 1a, Supplementary Table 2; *t*-test: $p = 0.022$; $r^2 = 0.29$, $p = 0.04$). These $\delta^{11}B$ values translate into pH_{cf} that are slightly lower (but not statistically significant) in the corals from sites with $\Omega_{sw} < 2$ with an average internal pH_{cf} of 8.46 (±0.03 sem) compared to 8.54 (±0.01 sem) at the control sites (*t*-test: $p = 0.085$, Fig. 1b, Supplementary Table 2). The pH_{cf} difference between the corals is relatively small (0.08 pH units) compared to the difference in environmental seawater pH_{sw} of ~0.54 pH units between the sites. Hence, compared to pH_{sw} in their surrounding environment, corals at the ojo centres maintained a higher pH gradient between seawater and the calcifying fluid (ΔpH) in comparison to corals at control sites (Fig. 1c, Supplementary Table 2; *t*-test: $p = 0.002$, $r^2 = 0.89$, $p < 0.001$).

Skeletal B/Ca, thus DIC_{cf} and $CO_3^{2-}{}_{cf}$ as a function of Ω_{sw}. Changes in coral skeletal B/Ca were determined along with $\delta^{11}B$. This ratio varied between 442 and 721 μmol mol^{-1} and did not significantly correspond to Ω_{sw} (Fig. 2a, $p = 0.86$). Using the $\delta^{11}B$ and B/Ca skeletal proxies together to constrain the carbonate system at the site of calcification suggests an elevation of $CO_3^{2-}{}_{cf}$ not only due to shifts in internal pH_{cf} but also due to an increase in DIC_{cf} (Supplementary Table 2, Fig. 2b). The ratios of DIC_{cf}/DIC_{sw} —a measure of the upregulation of DIC_{cf} compared to seawater—were significantly higher at the control sites than at the low Ω_{sw} sites (Fig. 2c, Supplementary Table 2; $p = 0.036$, $r^2 = 0.33$, $p = 0.029$). This is mainly due to the higher than ambient DIC_{sw} (Supplementary Table 1) at the ojos because the DIC_{cf} did

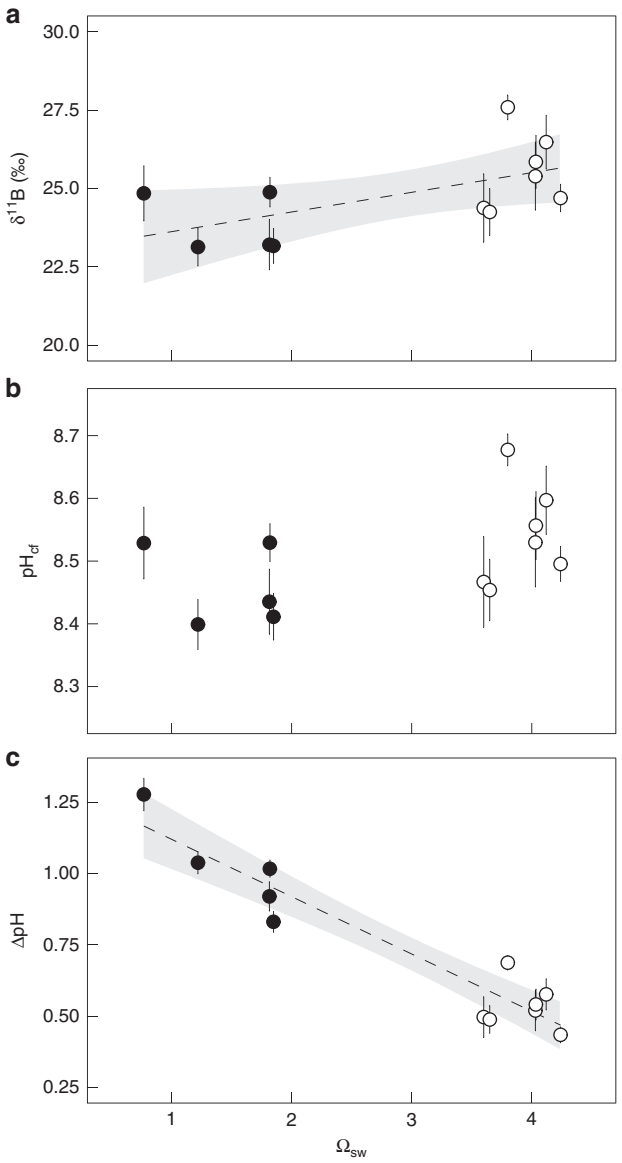

Fig. 1 *Porites astreoides* internal pH_{cf} regulation based on skeletal proxies. Coral skeletal $\delta^{11}B$ signature **a** from naturally different seawater aragonite saturation state (Ω_{sw}) sites were translated into **b** internal calcifying fluid pH (pH_{cf}) and **c** pH up-regulation intensity (ΔpH). Circles represent values for each individual coral colony (mean ± confidence interval). Filled and non-filled symbols denotes the different locations: filled are the centres of the ojos with lower Ω_{sw} and non-filled the control high Ω_{sw} site. Dashed line represents regression line for site-specific significant different values in $\delta^{11}B$ and ΔpH with Ω_{sw} ($r_{adj}^2 = 0.29$, $p = 0.04$, $r_{adj}^2 = 0.88$, $p < 0.001$, respectively) and grey area denotes the 95% confidence band. Individual values are mean ± 95%-confidence interval

not vary significantly between the sites (Supplementary Fig. 1, Supplementary Table 2; $p = 0.85$).

Changes in calcification conditions and calcification rates. We applied a bio-inorganic model (IpHRAC model from McCulloch and colleagues[19], see the "Methods" section) to calculate average Ω_{cf} and associated relative calcification rates using our proxy data. We used the combined pH_{cf} and the B/Ca-derived DIC_{cf} concentration at the site of calcification for corals from both ojo and control sites. With this bio-inorganic model both Ω_{cf} (from 16.1 ± 0.3 sem to 13.1 ± 0.7 sem, Fig. 3a; $p = 0.042$) and calcification rates (from 1.0 ± 0.09 sem to 0.54 ± 0.09 sem; $p = 0.036$) decreased with decreasing Ω_{sw} and correlated well with the observed calcification response previously reported for these corals[11] (Fig. 3b). 41% of the variation in measured net calcification rates can be explained by internal changes in Ω_{cf} derived from the geochemically determined calcifying conditions (Fig. 4a; $r^2_{adj} = 0.41$, $p = 0.011$). The internal calcifying fluid parameters are clearly distinct between corals from the different field sites, strongly indicating a combined effect of DIC_{cf} and pH_{cf} modulation on *P. astreoides* calcification performance (Fig. 4b).

Discussion

Coral calcification is one of the most fundamental processes in reef ecosystems and is essential for reef accretion and ecosystem diversity; however, calcification may be impacted by changes in seawater carbonate chemistry. Although corals are sensitive to changes in ocean carbonate chemistry[15], the underlying physiological mechanisms that determine vulnerability are far from understood. Natural sites with low aragonite saturation that select for genotypes that can calcify under such conditions and permit decade-long developmental acclimation to changes in Ω_{sw} are invaluable model systems for understanding the resilience of corals and coral calcification processes. Here we reveal that corals grown for their entire lifetime at low aragonite saturation conditions in their natural environment, at ojos in the Caribbean, exert strong control on both pH_{cf} and DIC_{cf}, thereby modulating $CO_3^{2-}{}_{cf}$, Ω_{cf}, and calcification rate. At the calcification site, both parameters that control Ω_{cf} (pH_{cf} and DIC_{cf}) decreased only slightly along the ambient Ω_{sw} gradient in which the analysed corals live, highlighting the strong control of *Porites asteroids* corals over the biomineralization process. Yet the combined change in pH_{cf} and DIC_{cf} corroborate the observed decline in calcification rate along the environmental gradient (Fig. 4b). Interestingly, at this field site ojos with low Ω_{sw} had elevated DIC_{sw}, but this did not result in higher DIC_{cf} concentrations in the calcifying fluids, indicating a decoupling of internal and external DIC concentrations. This indicates that corals have significant control over the carbonate chemistry of the calcifying fluid, likely mediated by bicarbonate transporters (NBC, SLC4 family of ion transporters) that are localised in the calicoblastic epithelium, as well as other, not yet identified acid–base relevant transporters[35]. Carbonate chemistry at the calcification site clearly differs between coral growing at the control and ojo locations. The difference explains 41% of the observed difference in calcification rate; however, it still leaves 59% of the variation in calcification rate unexplained (Fig. 4b).

In our study, we took advantage of the inherent conditions of this submarine springs system, including the strong environmental fluctuations and the fact that carbonate chemistry is controlled by saline groundwater discharge, allowing us to provide new facets on drivers of coral calcification in natural settings affected by ocean acidification. In the subsequent discussion we will outline the novel insights we derive from the observed internal carbonate chemistry conditions at this natural low Ω_{sw} site, discuss potential mechanisms that control calcification rates, add to the ongoing discussion on how seawater carbonate chemistry affects regulations of internal conditions at the site of calcification (e.g. ref. [23]), and emphasise the importance of deciphering internal calcium regulation[36–38].

The ability of organisms to modify pH_{cf} reflects the strong effect of intracellular biological processes on coral calcification and is manifested in skeletal isotopic composition. The control of pH_{cf} represents one mechanism to counter external seawater conditions[39]. The boron isotopic-derived pH_{cf} values we report are similar to those reported in other studies for *Porites*[25–27]. The

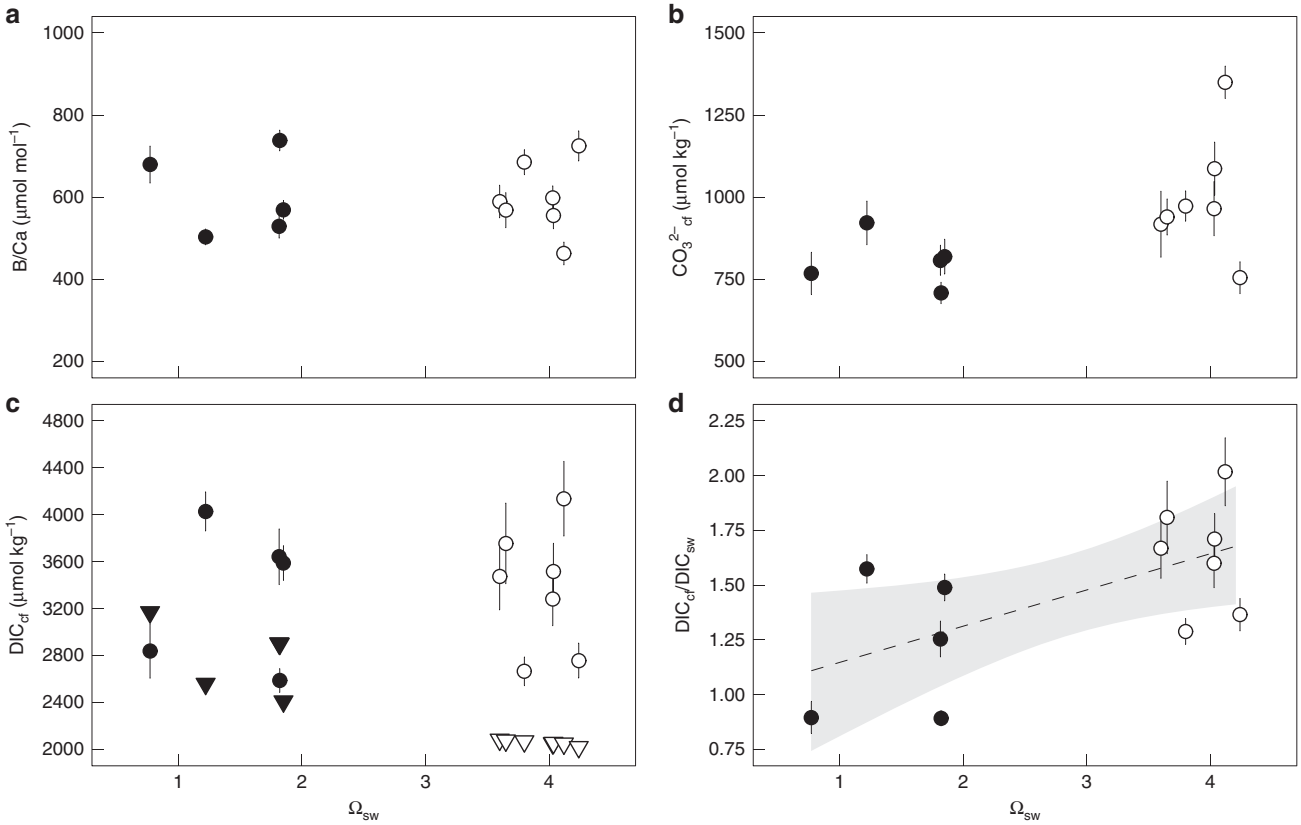

Fig. 2 *Porites astreoides* internal CO_3^{2-} and DIC_{cf} based on skeletal proxies. Coral skeletal B/Ca ratio **a** from naturally different seawater aragonite saturation state (Ω_{sw}) sites were translated into internal calcifying carbonate ion concentration (CO_3^{2-}) values **b** and dissolved inorganic carbon (DIC_{cf}) concentration, as well as upregulation compared to seawater (DIC_{cf}/DIC_{sw}) (**c**, **d** respectively). Circles represent values for each individual coral colony (mean ± confidence interval). Filled and non-filled symbols denotes the different locations: filled are the centres of the ojos with lower Ω_{sw} and non-filled the control high Ω_{sw} site. Triangles in **c** represent seawater DIC_{sw} concentrations. Dashed line represents regression line for site-specific significant different values for DIC_{cf}/DIC_{sw} with Ω_{sw} ($r_{adj}^2 = 0.33$, $p = 0.029$) and grey area denotes the 95% confidence band. Individual values are mean ± 95%-confidence interval

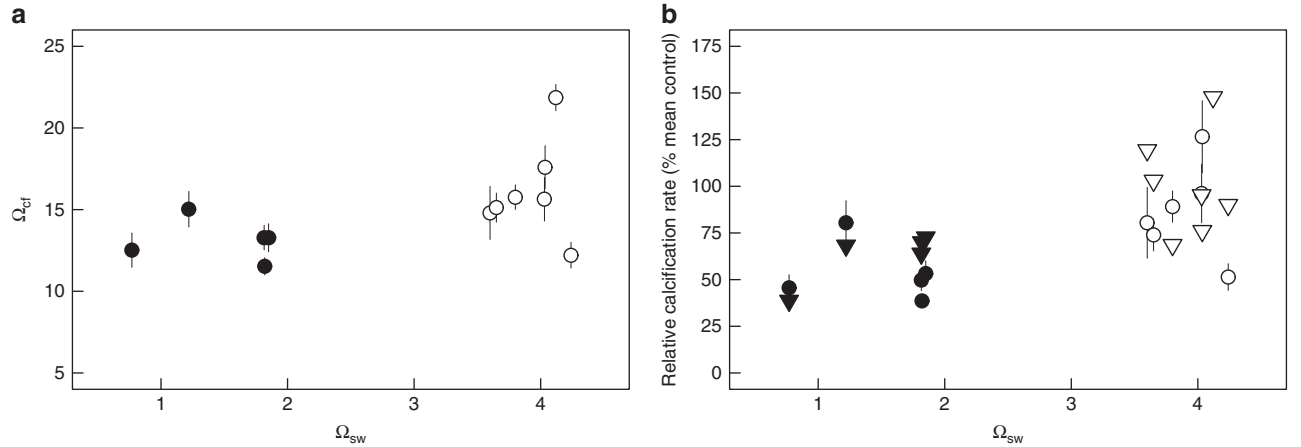

Fig. 3 Growth response of *Porites astreoides* corals. The modelled growth response displays relative changes in calcification rate (relative calcification rate = mean control/individual colony). Calcification rates were calculated following the IpHRAC model[19] (internal pH regulation and abiotic calcification: Calcification = $k^*(\Omega_{cf}-1)^n$) with calcifying fluid aragonite saturation state (Ω_{cf}) was calculated from the average internal calcifying fluid pH (pH_{cf}) of individual colonies and the dissolved inorganic carbon (DIC_{cf}): in **a** dependent variable Ω_{cf} is based on DIC_{cf} and pH_{cf} and **b** depicts the respective calculated calcification rates. Circles represent values for each individual coral colony (mean ± confidence interval). Filled and non-filled symbols denotes the different locations: filled are the centres of the ojos with lower seawater aragonite saturation state (Ω_{sw}) and non-filled the control high Ω_{sw} site. We compared calculated values with measured data[11] (for better comparison also calculated as relative rate, open triangles). Individual values are mean ± 95%-confidence interval

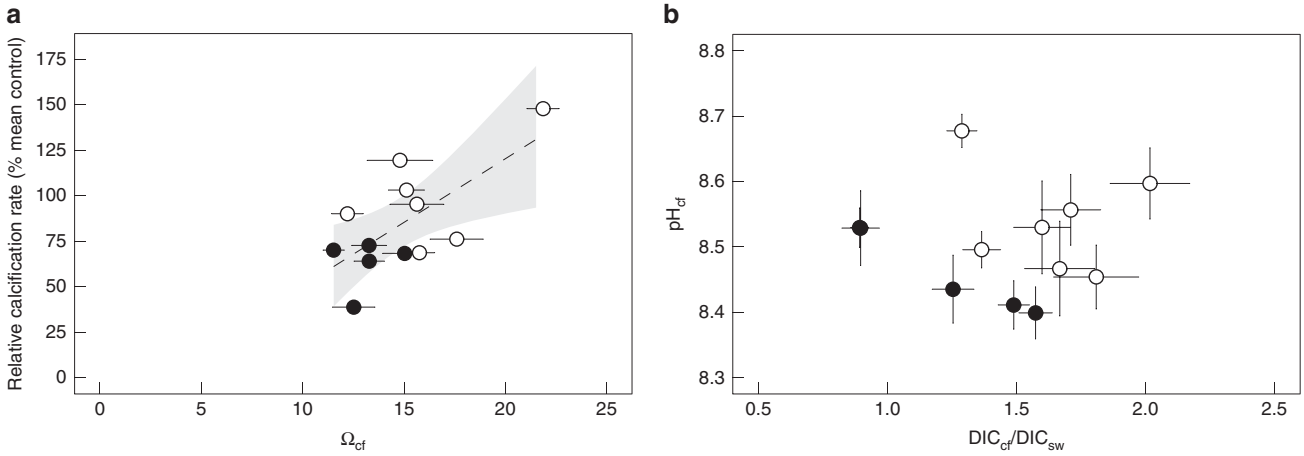

Fig. 4 Internal calcification conditions in *Porites astreoides*. **a** Calcifying conditions were used to calculate aragonite saturation state at the site of calcification (Ω_{cf}) and related to the measured growth rate of the individual corals[11]. **b** Calcification conditions as internal calcifying fluid pH (pH_{cf}) and dissolved inorganic carbon ratio of calcifying fluid to seawater (DIC_{cf}/DIC_{sw}) was determined for 12 *Porites astroides* coral colonies collected from sites with naturally different seawater aragonite saturation state (Ω_{sw}). Circles represent values for each individual coral colony (mean ± confidence interval). Filled and non-filled symbols denotes the different locations: filled are the centres of the ojos with lower Ω_{sw} and non-filled the control high Ω_{sw} site. Dashed line represents regression line for relative calcification rate with Ω_{cf} ($r_{adj}^2 = 0.41$, $p = 0.015$) and grey area denotes the 95% confidence band. Individual values are mean ± 95%-confidence interval

sensitivity of pH_{cf} to changes in the environmental pH_{sw}, however, differed between the different studies, as the environments the corals originated from were distinct[27,40]. All studies observed that pH_{cf} stays within a narrower range (8.2–8.6) compared to large changes in seawater pH_{sw}. They all highlight the generally strong control corals exert on pH_{cf}. Despite this capacity for regulation, however, the observed pH_{cf} was lower at lower Ω_{sw} (e.g. refs. [20,25,28,41]). Irrespective of whether corals maintained high pH_{cf}, the corals exposed to low Ω_{sw} maintained a higher proton gradient at lower pH_{sw} (Fig. 2b). A potential driving force that fosters acclimation to various changes a coral may experience is the environmental history corals have been exposed to during their lifetime[31]. For example, pH homoeostasis—the maintenance of internal pH_{cf} irrespective of the external seawater pH_{sw}—was observed in corals that live in a highly dynamic naturally variable environment[5,42]. The underlying assumption is that these corals are better able to buffer external changes by exerting a stronger control over the calcifying fluids or by better exploiting times of favourable conditions[27,40]. Although the ojos represent a highly dynamic system[33,43,44], coral performance measured in terms of net calcification was lower at these sites relative to the same species collected at control sites at the same location. Here, lifelong exposure to variable and persistently low Ω_{arag} (<2) did not lead to full acclimation[11]. It is likely that there is a critical Ω_{arag} threshold beyond which corals are no longer able to fully compensate for external acid–base changes. Such a critical threshold has been observed for corals grown at a Papua New Guinea CO_2 seep site, where pH_{cf} homoeostasis was only found for pH_{sw} of >7.8 and Ω_{sw} of >2.3. Beyond that, pH_{cf} could not reach the same values as those under control conditions, and likely the coral's physiological limit to compensate for changes was reached[40]. This lack of ability to fully compensate for the lower pH_{sw} may be responsible for the slight differences in pH_{cf} observed in this study.

The use of our dual geochemical proxy data to model coral growth (e.g. IpHRAC[19,30]) allowed us to further pinpoint potential mechanisms of how external seawater conditions affect internal calcifying conditions and ultimately skeletal growth. Calcification was once thought to be a passive diffusion process of seawater that brings external DIC to the site of calcification (potentially gaining DIC from metabolic CO_2 by passing through the paracellular pathways)[45] and by active ion transporters[46] that result in an elevation of pH_{cf}, thereby facilitating precipitation. At our study sites, DIC_{sw} is significantly higher at the low Ω_{sw} sites (in average 2790 μmol kg^{-1} compared to control average DIC_{sw} of 2050 μmol kg^{-1}) allowing us to decipher the role of external DIC_{sw} in modulating calcification regulation processes. If corals modify internal DIC_{cf} by simply up-regulating DIC_{cf} from the external concentrations baseline, we would expect higher DIC_{cf} values for the ojo corals where DIC_{sw} is higher. Under such assumption the elevated DIC_{cf} compensates for the slightly lower pH_{cf} effect on Ω_{cf} and calcification rates would essentially be similar between sites (Supplementary Fig. 1). However, our data clearly demonstrate that DIC_{cf} is not directly linked to external concentrations and can differ significantly from that of seawater[22,30,47] (reported DIC_{cf}-upregulation values range from 1.6 to 3.2[30,38], with the ojos corals at our sites at the lower end), and this impacts Ω_{cf} (more precisely CO_3^{2-}) and calcification. A recent study under laboratory conditions with *Stylophora pistillata*[23] observed that changes in DIC_{sw} concentration modulates internal pH_{cf} regulation, with higher external DIC_{cf} facilitating higher internal pH_{cf}, resulting in a clear correlation between seawater DIC_{sw}/H^+_{sw} and pH_{cf}. Since DIC_{sw} at the ojos is significantly higher than at the control sites, one could expect this to compensate reduced pH_{cf} up-regulation induced only due to changes in seawater pH_{sw}. Yet we do not see a strong correlation between pH_{cf} and seawater DIC_{sw}/H^+_{sw}, suggesting different drivers for Ω_{cf} regulation in *P. astreoides* compared to those observed in *S. pistillata*[23]. Nevertheless, the change in pH_{cf} and the limited ability to upregulate DIC_{cf} at the ojos corroborates the observed calcification rate decrease of corals at the ojos. However, these parameters may not be the only drivers for the decline in growth. Recent studies identified internal calcium (Ca^{2+}_{cf}) regulation as an additional player in coral calcification responses and emphasised that regulation of Ca^{2+}_{cf} can contribute to a corals' resistance to future ocean changes[36–38,48]. In this sense, the good agreement of our model with the observed calcification response may imply that internal average steady-state calcium concentrations (Ca^{2+}_{cf}) at the ojos are lower by some proportion that is related to the pH_{cf} changes, since our model based on pH_{cf} and

$CO_3^{2-}{}_{cf}$ can explain only 41% of the observed calcification decline. This suggests a strong link between $Ca^{2+}{}_{cf}$ and pH_{cf} and supports the idea of a plasma-membrane Ca-ATPase ([49], but see ref. [50]) responsible for pH_{cf} regulation. However, it is possible that pH_{cf} and $Ca^{2+}{}_{cf}$ were both regulated by additional and/or different ion transport mechanisms (e.g. potentially ion exchangers, Ca^{2+}-channels)[50,51].

The present study also indicates that the acclimation process in different corals encompass some degree of flexibility in terms of the relative role of pH_{cf} and DIC_{cf} regulation in increasing the Ω_{cf}, with some individuals compensating by adjusting their internal pH_{cf} and others primarily by DIC_{cf} modulation. This may also be true of the role of $Ca^{2+}{}_{cf}$ upregulation. The relative amount, source, and transportation pathways of DIC, H^+ and Ca^{2+} to the site of calcification are still not fully understood[52] and transport processes may differ between different coral species and even individual corals of the same species. Another potential driver for the observed differences among studies could be the number and type of symbionts the corals are hosting. Corals at the ojos harbour a higher density of symbionts[53] that may potentially account for the higher energy demands for pH_{cf} upregulation resulting in the relatively small difference in the internal conditions (pH_{cf}, DIC_{cf}) we see. Recent work provided the first evidence that coral symbionts (e.g. by modulating the chemical microenvironment within the diffusive boundary layer surrounding the coral that may buffer external changes[54]) and host genotypes can jointly affect coral calcification rates[55]. Similarly, possible interactions with the microbiome (e.g. restructuring of the corals microbiome[56]) or changes in energy acquisition and allocation processes to overcome environmental gradients[57,58] can affect coral growth. Environmental factors may also affect pH_{cf} and DIC_{cf} explaining some of the observed differences between the ojo and ambient corals at our study site. Studies have shown that a decrease in pH_{cf} and DIC_{cf} is associated with increasing temperature[38], yet at our sites the temperatures at the ojos is actually lower, on average, than at control sites. Salinity might also influence regulation processes, yet the measured average values (32.2 psu) as well as the salinity range measured (26–36 psu)[44] at the springs can be tolerated by corals and the long-term exposure to such conditions may have allowed them to develop mechanisms to better cope and adapt to this variable environment[59]. Overall, these environmental and biological parameters may be responsible for the observed internal conditions in the calcifying fluid but likely also affect rates of processes that ultimately affect calcification, and thus contribute to the unexplained component in our relationship between calcification and the geochemically derived DIC_{cf} and pH_{cf}. Our geochemical model approach assumes steady-state equilibrium conditions; however, the rates of the various transport processes involved in regulating the chemistry of the calcifying fluid will ultimately dictate the calcification response[60]: these rates may differ between individual coral genotypes, further contributing to the offsets between the model output and observations.

In this study, we utilised a dual geochemical proxy approach ($\delta^{11}B$ and B/Ca) to constrain calcifying fluid carbonate chemistry in *P. astreoides* corals that spent their entire life (decades) under acidified low Ω_{sw} conditions. We found that at the pH_{cf} for corals at the low Ω_{sw} was slightly lower than at the ambient conditions indicating inability to achieve optimal calcification conditions. We also determined that pH_{cf} and DIC_{cf} are independently regulated and corroborated the calcification response in *P. astreoides* at this site. The study provides new insights into calcification responses of *P. astreoides* under changing environmental conditions and sheds light on the potential of corals to acclimate[30,41,47,61,62]. Using the geochemical proxies in combination with the bio-inorganic model brought forward by McCulloch et al. [30], we could explain 41% of the variability in coral growth rates along a Ω_{sw} gradient. The variability which is not explained indicates that additional physiological and environmental processes contribute to the control of calcification rates in natural environments. This provides promising new avenues towards studying acclimation and adaptation potential of long-lived marine invertebrates such as corals.

Methods

Site description and coral core collection. Cores from colonies of *P. astreoides* were collected at the ojos—natural springs of low-pH water—in the National Maritime Park at Puerto Morelos, Mexico (see refs. [11,43] for more details). Five cores were drilled in close proximity to the low pH discharge and seven cores were drilled from control sites outside the ojos discharge influence (~2–5 m away). After collection, cores were dried at 50 °C before further analysis. Water chemistry was measured at the different sites (summarised in Supplementary Table 1 and for more details see refs. [11,33,43,44,63,64]) and used to calculate carbonate chemistry (see Supplementary Table 1). In general, corals were collected from sites that have similar light conditions, differ marginally in temperature (<1 °C lower at the ojos averaged over all seasons with temperatures cooler than ambient in summer and slightly warmer in winter), have consistently lower salinity (2–4 units lower than ambient), and are considerably different in Ω_{sw} (Supplementary Table 1)[11,44]. We note that these submarine springs are not perfect analogues for future ocean acidification. Specifically, the conditions creating low-pH seawater at the ojos differ from those of the ocean acidification scenario as the high CO_2 in the discharging water at the ojos is derived from brackish water that has interacted with soil and limestone. The spring water is characterised by lower pH, higher DIC, higher TA but similar calcium (Ca^{2+}) concentration compared to the ambient conditions away from the spring influence. The corals at these ojos are constantly exposed to these discharging water (Supplementary Table 1), as discussed in detail in refs. [11,43,44], and they represent settings with persistent low Ω_{sw}. In particular, because such conditions have persisted at the ojo discharge sites at least since the last deglaciation (~18,000 years ago[65]) the corals at these sites were exposed to low Ω_{sw} for their whole life span, potentially allowing enough time for acclimation. Moreover, it is quite likely that strong selection processes have resulted in successful colonisation of the ojos by a fraction of the coral population that is better adapted to low pH_{sw} and high CO_2.

Water samples were also taken for seawater boron concentrations (measured on a ICP-MS Finnigan Element XR following Krupinski and colleagues[66]; ~430 ± 8 µM, with no difference between ojos and control) and a boron isotopic composition ($\delta^{11}B_{sw}$) of 39.15 (1sd = 0.12; $n = 3$) for the control site and 38.85 (1sd = 0.17; $n = 5$) for the low pH ojos. Boron isotopic samples were analysed on a Neptune multi-collector inductively coupled mass spectrometer at National Cheng Kung University, Taiwan, using the standard-sample-standard bracketing technique[67]. The boric acid standard IAEA-B-1 was used as the reference standard (e.g. 39.77‰) to determine the $\delta^{11}B$ of the samples, reproducibility (±0.25‰).

Sample preparation and geochemical analysis. Collected coral cores were cut in half. One half was bleached for 24 h, thoroughly washed with milli-Q and dried overnight at 50 °C. Subsequently, the slab surfaces were carefully ground (Struers Silicon carbide grinding paper SiC 500–4000) and briefly polished (Struers DiaPor Dur 9 µm polishing suspension) in preparation for boron analysis using a Struers TegraPol-21 with TegraForce-5 head (Grinder and Polisher). The $\delta^{11}B$ and B/Ca composition was measured simultaneous by laser ablation multi-collector inductively coupled plasma mass spectrometer (Thermo Fisher MC-ICP-MS AXIOM, connected to a UP193fx laser ablation system of New Wave Research, equipped with an excimer 193 nm laser). The measurement procedure followed Fietzke et al.[68] and Wall et al.[40] with slight modifications. Specifically, we used Multiplier and Faraday cups simultaneously to collect data for B^{10} and B^{11} (both on multiplier) as well as C^{12} (Faraday cup). This allows us to derive B/C and $\delta^{11}B$ from the same skeletal material. Similar to previous work the cones were cleaned on a regular basis (every 2–4 days). The tubes going from the ablation cell to the plasma torch were checked for material deposition and cleaned by high flow rates overnight and/or mobilisation of the debris by increased flow rates transporting it out of the tubes. Prior to each measurement session the standard and samples were pre-ablated to remove surface contaminations (spot size used was one size bigger than during analysis). A standard-sample-bracketing method was used. The data of one measurement session contained 5–6 brackets. Both C^{12} and the variation of the standard (NIST SMR610) for each session were used to check for instrument stability and contaminations. Sessions were repeated when the standard drift was higher than the internal reproducibility of the standards (2 SD of the session on the standards). Twenty individual laser tracks (25 × 500 µm) were placed as close as possible to the edge of the skeletal section (expecting to mainly ablate fibres and avoid centres of calcification (COC)), far enough away to avoid ablation through the skeletal part. Yet COC areas may not have been completely avoided. To account for this we: (a) subsequently screened the individual tracks for abnormalities in C^{12} indicative of either ablation through the coral skeletal part (since the underlying skeletal depth is unknown from the surface view, this screening is completed

afterwards) or increased organics and excluded this parts from analysis, and (b) aimed for 20 tracks of ~25 × 500 × 20 µm on all individuals to have a representative $\delta^{11}B$ dataset per individual. By this approach we expect to cover a representative sample set and minimise the natural intra-skeletal variability and cover similar proportions in each of the different corals (assuming that COC to fibre ratio in coral grown under various environmental conditions stays constant). The accuracy of our $\delta^{11}B$ measurements has been checked by repeated analyses of *Porites* coral standard Jcp-1 and NIST SRM610, measured against a pellet of primary boron standard NBS951 (boric acid) (see Supplementary Fig. 2).

$\delta^{11}B$ determination. The data reduction followed Fietzke et al.[68]. This yields one $\delta^{11}B$ value per sample and session with an average precision of <1‰ (1 SD) for ~1.7 µg of carbonate sample. A minimum of 15 and up to 20 values of $\delta^{11}B$ spread over the core surface in the upper few mm of each coral colony (below the tissue, representing ~1 year of growth) were measured to obtain a representative data set per sample. The data set reflects the high variability in $\delta^{11}B$ for a single colony, and replicates were averaged afterwards to yield values that reflect the mean $\delta^{11}B$ value, hence the mean internal calcification conditions (see below).

B/Ca determination. B/C elemental ratios have been determined simultaneously with the boron isotope ratios via LA–MC–ICP–MS. Boron isotope data (^{10}B and ^{11}B) have been collected using a pair of ion counters, while carbon (^{12}C) had been determined using a Faraday cup. B/C data are based on the integrated boron intensities ($^{10}B + {}^{11}B$) divided by the ^{12}C intensity. The calibration (conversion from intensity ratios to concentration ratios) has been done using a natural *L. pertusa* coral sample covering a B concentration range of about 450–950 µmol/mol, which had been determined before using LA–ICP–MS relative to standard NIST-SRM610 using ^{43}Ca as internal standard. This calibration procedure resulted in: B/C [µmol/mol] = 78,800 × B/C [cps/cps]; (cps—counts per second, ion beam intensity). We used stoichiometric ratio of C/Ca = 1 as approximation for natural carbonates and translated B/C ratios in B/Ca [µmol/mol] ratios.

$\delta^{11}B$ as internal pH_{cf} proxy. All $\delta^{11}B$ values were translated into internal pH_{cf} following Eq. (1) with a seawater $\delta^{11}B_{sw}$ of 38.85 for ojo centres and 39.15 for control sites, a fractionation factor (α_B) of 1.0272[69] and pK^*_B averaged for the two sites (see Supplementary Table 1).

$$pH_{cf} = pK_B - \log\left[\left(\delta^{11}B_{sw} - \delta^{11}B\right)/\left(\alpha_B * \delta^{11}B - \delta^{11}B_{SW} + 1000 * (\alpha_B - 1)\right)\right] \quad (1)$$

Following the method in Trotter and colleagues[24] the superimposed physiological pH control was calculated with the equation:

$$\Delta pH = pH_{cf} - pH_{sw} \quad (2)$$

and related to the seawater aragonite saturation state (Ω_{sw}) to quantify the extent of the physiological control on the internal pH_{cf}.

We note here, that the local variability in carbonate chemistry at the ojos and hence, associated changes in pK_B and seawater $\delta^{11}B$ can add some uncertainty to the derived pH_{cf} and overestimate or underestimate its actual value. To test the sensitivity to changes in pK_B we used our dataset and recalculated pH_{cf} values. We applied a range of seawater $\delta^{11}B_{sw}$ that encompasses the average measured $\delta^{11}B_{sw}$ per site but also seawater isotopic composition beyond this level ranging from 38.55‰ to 39.45‰ and recalculated pH_{cf} (Supplementary Fig. 3a). This allowed us to decipher the combined role of site specific pK_B and seawater $\delta^{11}B_{sw}$ for a range of skeletal $\delta^{11}B$ (Supplementary Fig. 3b). In general, the $\delta^{11}B$-derived pH_{cf} decreases slightly with increasing seawater $\delta^{11}B$. Changes in seawater $\delta^{11}B_{sw}$ in the corals surrounding will either over or underestimate pH_{cf} and calculated changes in pH_{cf} range from 0.019 to 0.023 pH units per 0.3 change in $\delta^{11}B_{sw}$ (Supplementary Fig. 3c the average difference between our sites; or change from 0.056–0.065 for the entire seawater $\delta^{11}B_{sw}$ range tested). Compared to the pH_{cf} range (8.2–8.8) derived from individually measured skeletal $\delta^{11}B$ values such changes are minor (Supplementary Fig. 3a; in contrast to the individual coral's pH_{cf} standard deviation of 0.04–0.13, Supplementary Table 2).

B/Ca as $CO_3^{2-}{}_{cf}$ and DIC_{cf} proxy. All individual B/Ca data were used to estimate $CO_3^{2-}{}_{cf}$ based on the $\delta^{11}B$-derived pH_{cf} data and further used to calculate the DIC_{cf} following the approach of McCulloch et al.[30]. This allows to use the following simplified relationship to determine the $CO_3^{2-}{}_{cf}$ concentration from B/Ca[30]:

$$\left[CO_3^{2-}\right]_{cf} = \left[B(OH)_4^-\right]_{cf} * K_D^{B/Ca}/(B/Ca) \quad (3)$$

and the distribution coefficient is determined for synthetic aragonite and follows the equation:

$$K_D^{B/Ca} = 0.00297\exp\left(-0.0202\left[H^+\right]_{cf}\right) \quad (4)$$

based on the internal pH_{cf}[29,30]. Both pH_{cf} and $[CO_3^{2-}]_{cf}$ are then used to calculate DIC_{cf}.

Modelling calcification rate using internal pH_{cf} and DIC_{cf}. Calcification rate (G) was calculated following McCulloch et al.[19] IpHRAC model:

$$G = k * (\Omega_{cf} - 1)^n \quad (5)$$

The calcification response was calculated with the temperature-dependent rate law constant k and reaction order constant n (applying the equations given in McCulloch et al.[19]: $k = -0.0177*T^2 + 1.47*T + 14.9$ and $n = 0.0628*T + 0.0985$). The individual average temperature data for the different sites were used (Table S1).

For a sole pH-regulation-based model we used seawater DIC concentration DIC_{sw} that were measured at the different sites the individual corals were collected (see Table S1). Aragonite saturation state at the site of calcification (Ω_{cf}) was calculated from pH_{cf} and DIC_{cf} using seacarb. We first followed recent approaches[19,20] by setting DIC_{cf} equivalent to double DIC_{sw}[19]. In a second step an advanced bio-inorganic model used both geochemically determined calcification parameters to calculate Ω_{cf}. For the seacarb (R) calculations we used the measured average salinity and temperature for the different sites. We assumed $[Ca]^{2+}$ concentrations that equals seawater values to calculate Ω_{cf}.

Both modelled calcification rates were plotted against the measured calcification rates[11], by converting them into relative rates and setting the control site as 1 (or 100%[19]).

Statistical analysis. Statistical analysis of the geochemical proxies and derived internal calcification conditions was performed by comparing the two treatment groups (control conditions vs. reduced aragonite saturation state at the centres of the ojos) using Welch's t-test (unequal sample numbers). To understand how well the internal calcification conditions (Ω_{cf}—a combined value of both internal pH_{cf} and DIC_{cf}) can explain measured changes in net calcification rate we applied simple linear models regressing model-derived relative growth as a function of internal Ω_{cf}. Similarly, changes in geochemical proxies as well as internal conditions were regressed to decipher correlation between these parameters and potential driving forces explaining changes in net calcification rate along the natural environmental seawater Ω_{sw} gradient[20].

Data analysis and visualisation was done with R Studio version 3.0.1 (R Development Core Team, 2015).

Data availability

All coral geochemical data and derived calcification conditions are available as Supplementary data file.

Received: 28 October 2018 Accepted: 10 July 2019
Published online: 08 August 2019

References

1. Fabricius, K. E. et al. Losers and winners in coral reefs acclimatized to elevated carbon dioxide concentrations. *Nat. Clim. Chang.* **1**, 165–169 (2011).
2. De'ath, G., Lough, J. M. & Fabricius, K. E. Declining coral calcification on the Great Barrier Reef. *Science* **323**, 116–119 (2009).
3. Albright, R. & Langdon, C. Ocean acidification impacts multiple early life history processes of the Caribbean coral *Porites astreoides*. *Glob. Chang. Biol.* **17**, 2478–2487 (2011).
4. Anthony, K. R. N., Kline, D. I., Diaz-Pulido, G., Dove, S. & Hoegh-Guldberg, O. Ocean acidification causes bleaching and productivity loss in coral reef builders. *Proc. Natl Acad. Sci. USA* **105**, 17442–17446 (2008).
5. Venn, A. A. et al. Impact of seawater acidification on pH at the tissue–skeleton interface and calcification in reef corals. *Proc. Natl Acad. Sci. USA* **110**, 1634–1639 (2013).
6. Langdon, C. et al. Effect of calcium carbonate saturation state on calcifcation rate of an experimental coral reef. *Glob. Biogeochem. Cycles* **14**, 639–654 (2000).
7. Jokiel, P. L. et al. Ocean acidification and calcifying reef organisms: a mesocosm investigation. *Coral Reefs* **27**, 473–483 (2008).
8. Dove, S. G. et al. Future reef decalcification under a business-as-usual CO2 emission scenario. *Proc. Natl Acad. Sci. USA* **110**, 15342–15347 (2013).
9. Albright, R. et al. Reversal of ocean acidification enhances net coral reef calcification. *Nature* **531**, 362–365 (2016).
10. Albright, R. et al. Carbon dioxide addition to coral reef waters suppresses net community calcification. *Nature* https://doi.org/10.1038/nature25968 (2018).
11. Crook, E. D., Cohen, A. L., Rebolledo-vieyra, M., Hernandez, L. & Paytan, A. Reduced calcification and lack of acclimatization by coral colonies growing in areas of persistent natural acidification. *Proc. Natl Acad. Sci. USA* **110**, 11044–11049 (2013).
12. Shamberger, K. E. F. et al. Diverse coral communities in naturally acidified waters of a Western Pacific reef. *Geophys. Res. Lett.* **41**, 499–504 (2014).

13. Barkley, H. C. & Cohen, A. L. Skeletal records of community-level bleaching in Porites corals from Palau. *Coral Reefs* **35**, 1407–1417 (2016).
14. Goffredo, S. et al. Biomineralization control related to population density under ocean acidification. *Nat. Clim. Chang.* **4**, 593–597 (2014).
15. Chan, N. C. S. & Connolly, S. R. Sensitivity of coral calcification to ocean acidification: a meta-analysis. *Glob. Chang. Biol.* **19**, 282–290 (2013).
16. Strahl, J. et al. Physiological and ecological performance differs in four coral taxa at a volcanic carbon dioxide seep. *Comp. Biochem. Physiol. Part A* **184**, 179–186 (2015).
17. Castillo, K. D., Ries, J. B., Bruno, J. F. & Westfield, I. T. The reef-building coral Siderastrea siderea exhibits parabolic responses to ocean acidification and warming. *Proc. R. Soc. B* **281**, 20141856 (2014).
18. Ries, J. B., Cohen, A. L. & McCorkle, D. C. Marine calcifiers exhibit mixed responses to CO2-induced ocean acidification. *Geology* **37**, 1131–1134 (2009).
19. McCulloch, M., Falter, J., Trotter, J. & Montagna, P. Coral resilience to ocean acidification and global warming through pH up-regulation. *Nat. Clim. Chang.* **2**, 623–627 (2012).
20. Holcomb, M. et al. Coral calcifying fluid pH dictates response to ocean acidification. *Sci. Rep.* **4**, 5207 (2014).
21. Al-Horani, F., Al-Moghrabi, S. M. & de Beer, D. Microsensor study of photosynthesis and calcification in the scleractinian coral, *Galaxea fascicularis*: active internal carbon cycle. *J. Exp. Mar. Biol. Ecol.* **288**, 1–15 (2003).
22. Cai, W. et al. Microelectrode characterization of coral daytime interior pH and carbonate chemistry. *Nat. Commun.* 1–8 https://doi.org/10.1038/ncomms11144 (2016).
23. Comeau, S. et al. Coral calcifying fluid pH is modulated by seawater carbonate chemistry not solely seawater pH. *Proc. R. Soc. B* **284**, 20161669 (2017).
24. Trotter, J. et al. Quantifying the pH 'vital effect' in the temperate zooxanthellate coral *Cladocora caespitosa*: validation of the boron seawater pH proxy. *Earth Planet. Sci. Lett.* **303**, 163–173 (2011).
25. Hönisch, B. et al. Assessing scleractinian corals as recorders for paleo-pH: empirical calibration and vital effects. *Geochim. Cosmochim. Acta* **68**, 3675–3685 (2004).
26. Rollion-Bard, C., Chaussidon, M. & France-Lanord, C. Biological control of internal pH in scleractinian corals: implications on paleo-pH and paleo-temperature reconstructions. *C. R.-Geosci.* **343**, 397–405 (2011).
27. Georgiou, L. et al. pH homeostasis during coral calcification in a free ocean CO2 enrichment (FOCE) experiment, Heron Island reef flat, Great Barrier Reef. *Proc. Natl Acad. Sci. USA* **112**, 13219–13224 (2015).
28. Krief, S. et al. Physiological and isotopic responses of scleractinian corals to ocean acidification. *Geochim. Cosmochim. Acta* **74**, 4988–5001 (2010).
29. Holcomb, M., DeCarlo, T. M., Gaetani, G. A. & McCulloch, M. Factors affecting B/Ca ratios in synthetic aragonite. *Chem. Geol.* **437**, 67–76 (2016).
30. McCulloch, M. T., D'Olivo, J. P., Falter, J., Holcomb, M. & Trotter, J. A. Coral calcification in a changing world and the interactive dynamics of pH and DIC upregulation. *Nat. Commun.* **8**, 1–8 (2017).
31. Rivest, E. B., Comeau, S. & Cornwall, C. E. The role of natural variability in shaping the response of coral reef organisms to climate change. *Curr. Clim. Chang. Rep.* 1–11 https://doi.org/10.1007/s40641-017-0082-x (2017).
32. Fabricius, K. E., De'ath, G., Noonan, S. & Uthicke, S. Ecological effects of ocean acidification and habitat complexity on reef-associated macroinvertebrate communities. *Proc. R. Soc. B* **281**, 20132479 (2014).
33. Hofmann, G. E. et al. High-frequency dynamics of ocean pH: a multi-ecosystem comparison. *PLoS ONE* **6**, e28983 (2011).
34. Palumbi, S. R., Barshis, D. J., Traylor-Knowles, N. & Bay, R. A. Mechanisms of reef coral resistance to future climate change. *Science (80-.)* **344**, 895–898 (2014).
35. Zoccola, D. et al. Bicarbonate transporters in corals point towards a key step in the evolution of cnidarian calcification. *Sci. Rep.* **5**, 1–11 (2015).
36. DeCarlo, T. M., Comeau, S., Cornwall, C. E. & McCulloch, M. T. Coral resistance to ocean acidification linked to increased calcium at the site of calcification. *Proc. R. Soc. B* **285**, 20180564 (2018).
37. Ross, C. L., Schoepf, V., Decarlo, T. M. & McCulloch, M. T. Mechanisms and seasonal drivers of calcification in the temperate coral *Turbinaria reniformis* at its latitudinal limits. *Proc. R. Soc. B* **285**, 20180215 (2018).
38. Ross, C. L., DeCarlo, T. M. & Mcculloch, M. T. Environmental and physiochemical controls on coral calcification along a latitudinal temperature gradient in Western Australia. *Glob. Chang. Biol.* **25**, 431–447 (2019).
39. Allison, N. & Finch, A. A., EIMF. δ11B, Sr, Mg and B in a modern Porites coral: the relationship between calcification site pH and skeletal chemistry. *Geochim. Cosmochim. Acta* **74**, 1790–1800 (2010).
40. Wall, M. et al. Internal pH regulation facilitates in situ long-term acclimation of massive corals to end-of-century carbon dioxide conditions. *Nat. Publ. Gr.* 1–7 https://doi.org/10.1038/srep30688 (2016).
41. Schoepf, V., Jury, C. P., Toonen, R. J. & McCulloch, M. T. Coral calcification mechanisms facilitate adaptive responses to ocean acidification. *Proc. Biol. Sci.* **284**, 20172117 (2017).
42. Tambutté, E. et al. Morphological plasticity of the coral skeleton under CO2-driven seawater acidification. *Nat. Commun.* **6**, 7368 (2015).
43. Crook, E. D., Potts, D., Rebolledo-Yieyra, M., Hernandez, L. & Paytan, A. Calcifying coral abundance near low-pH springs: implications for future ocean acidification. *Coral Reefs* **31**, 239–245 (2012).
44. Paytan, A. et al. Reply to Iglesias-Prieto et al.: combined field and laboratory approaches for the study of coral calcification. *Proc. Natl Acad. Sci. USA* **111**, E302–E303 (2014).
45. Tambutte, E. et al. Calcein labelling and electrophysiology: insights on coral tissue permeability and calcification. *Proc. R. Soc. B* **279**, 19–27 (2012).
46. McConnaughey, T. A. & Whelan, J. F. Calcification generates protons for nutrient and bicarbonate uptake. *Earth-Sci. Rev.* **42**, 95–117 (1997).
47. Allison, N., Cohen, I., Finch, A. A., Erez, J. & Tudhope, A. W. Corals concentrate dissolved inorganic carbon to facilitate calcification. *Nat. Commun.* **5**, 5741 (2014).
48. Comeau, S., Cornwall, C. E., DeCarlo, T. M., Krieger, E. & Mcculloch, M. T. Similar controls on calcification under ocean acidification across unrelated coral reef taxa. *Glob. Chang. Biol.* **24**, 4857–4868 (2018).
49. Zoccola, D. et al. Molecular cloning and localization of a PMCA P-type calcium ATPase from the coral *Stylophora pistillata*. *Biochim. Biophys. Acta* **1663**, 117–126 (2004).
50. Barott, K. L., Perez, S. O., Linsmayer, L. B. & Tresguerres, M. Differential localization of ion transporters suggests distinct cellular mechanisms for calcification and photosynthesis between two coral species. *Am. J. Physiol. Regul. Integr. Comp. Physiol.* **309**, R235–R246 (2015).
51. Tresguerres, M. et al. Cell Biology of Reef-Building Corals: Ion Transport, Acid/Base Regulation, and Energy Metabolism. In *Acid-Base Balance and Nitrogen Excretion in Invertebrates* (eds. Weihrauch, D. & O'Donnell, M.) 193–218 (Springer International Publishing, 2017).
52. Allemand, D., Tambutté, É., Zoccola, D. & Tambutté, S. Coral calcification, cells to reefs. In *Coral Reefs: An Ecosystem in Transition SE-9* (eds. Dubinsky, Z. & Stambler, N.) 119–150 (Springer, Netherlands, 2011).
53. Martinez, A. et al. Species-specific calcification response of Caribbean corals after 2-year transplantation to a low aragonite saturation submarine spring. *Proc. R. Soc. B* **286**, https://doi.org/10.1098/respb.20190572 (2019).
54. Chan, N. C. S., Wangpraseurt, D., Kühl, M. & Connolly, S. R. Flow and coral morphology control coral surface pH: implications for the effects of ocean acidification. *Front. Mar. Sci.* **3**, 1–11 (2016).
55. Gold, Z. & Palumbi, S. R. Long-term growth rates and effects of bleaching in *Acropora hyacinthus*. *Coral Reefs* https://doi.org/10.1007/s00338-018-1656-3 (2018).
56. Morrow, K. M. et al. Natural volcanic CO2 seeps reveal future trajectories for host-microbial associations in corals and sponges. *ISME J.* **9**, 894–908 (2015).
57. Anthony, K. R. N., Hoogenboom, M. O., Maynard, J. A., Grottoli, A. G. & Middlebrook, R. Energetics approach to predicting mortality risk from environmental stress: a case study of coral bleaching. *Funct. Ecol.* **23**, 539–550 (2009).
58. Wall, C. B., Mason, R. A. B., Ellis, W. R., Cunning, R. & Gates, R. D. Elevated pCO2 affects tissue biomass composition, but not calcification, in a reef coral under two light regimes. *R. Soc. Open Sci.* **4**, 170683 (2017).
59. Kerswell, A. P. & Jones, R. J. Effects of hypo-osmosis on the coral *Stylophora pistillata*: nature and cause of ' low-salinity bleaching'. *Mar. Ecol. Prog. Ser.* **253**, 145–154 (2003).
60. Guo, W. Seawater temperature and buffering capacity modulate coral calcifying pH. *Sci. Rep.* **9**, 1189 (2019).
61. Comeau, S., Cornwall, C. E. & McCulloch, M. T. Decoupling between the response of coral calcifying fluid pH and calcification to ocean acidification. *Sci. Rep.* **7**, 1–10 (2017).
62. D'Olivo, J. P. & McCulloch, M. T. Response of coral calcification and calcifying fluid composition to thermally induced bleaching stress. *Sci. Rep.* **7**, 1–15 (2017).
63. Crook, E. D. et al. Recruitment and succession in a tropical benthic community in response to in-situ ocean acidification. *PLoS ONE* https://doi.org/10.1371/journal.pone.0146707 (2016).
64. Null, K. A. et al. Composition and fluxes of submarine groundwater along the Caribbean coast of the Yucatan Peninsula. *Cont. Shelf Res.* https://doi.org/10.1016/j.csr.2014.01.011 (2014).
65. Medina-Elizalde, M. & Rohling, E. J. Collapse of classic maya civilization related to modest reduction in precipitation. *Science (80-.)* **335**, 956–959 (2012).
66. Krupinski, N. B., Russell, A. D., Pak, D. K. & Paytan, A. Core-top calibration of B/Ca in Pacific Ocean Neogloboquadrina incompta and Globigerina bulloides as a surface water carbonate system proxy. *Earth Planet. Sci. Lett.* **466**, 139–151 (2017).
67. Wang, B.-S. et al. Direct separation of boron from Na- and Ca-rich matrices by sublimation for stable isotope measurement by MC-ICP-MS. *Talanta* **82**, 1378–1384 (2010).
68. Fietzke, J. et al. Boron isotope ratio determination in carbonates via LA-MC-ICP-MS using soda-lime glass standards as reference material. *J. Anal. Spectrom.* **25**, 1953 (2010).

69. Klochko, K., Kaufman, A. J., Yao, W., Byrne, R. H. & Tossell, J. A. Experimental measurement of boron isotope fractionation in seawater. *Earth Planet. Sci. Lett.* **248**, 276–285 (2006).

Acknowledgements

The research was funded by the German Federal Ministry for Education and Research project BIOACID II (Consortium 3: Natural CO2-rich reefs as windows into the future: Acclimation of marine life to long-term ocean acidification and consequences for bio-geochemical cycle, Grant number: 03F0655A), the Austrian Science Fund Schrödinger Fellowship (funding to M.W., FWF J3667-B25), and National Science Foundation (NSF) OCE-1040952, a University of California Institute for Mexico and the United States (UC-Mexus) grant (to A.P.), and NSF OCE-1041106. E.D.C. was funded through NSF-GFR and a EPA-STAR fellowships. All corals were collected under Secretaría de Agricultura, Ganadería, Desarrollo Rural, Pesca y Alimentación (SAGARPA) Permit DGOPA.00153.170111.-0051 and exported with a Convention on International Trade in Endangered Species (CITES) Permit MX52912.

Author contribution

M.W., J.F. and A.P. designed the experimental analyses. E.D.C. collected the samples. M. W. prepared the samples. M.W. and J.F. analysed the samples. E.D.C. and A.P. provided background data. M.W. analysed data. M.W., J.F., A.P. and E.D.C. were involved in the preparation of the manuscript.

Additional information

Supplementary Information accompanies this paper at https://doi.org/10.1038/s41467-019-11519-9.

Competing interests: The authors declare no competing interests.

Reprints and permission information is available online at http://npg.nature.com/reprintsandpermissions/

Peer review information: *Nature Communications* thanks Thomas DeCarlo and other anonymous reviewer(s) for their contribution to the peer review of this work. Peer reviewer reports are available.

Publisher's note: Springer Nature remains neutral with regard to jurisdictional claims in published maps and institutional affiliations.